Calibration-Free Fusion of Step Counter and Wireless Fingerprints for Indoor Localization

Suining He   S.-H. Gary Chan
Dept. of Computer Science and Engineering,
The Hong Kong University of Science and
Technology, Hong Kong, China
{sheaa, gchan}@cse.ust.hk

Lei Yu   Ning Liu
School of Software,
Sun Yat-sen University, Guangzhou, China
{yulei5@mail2, liuning2@mail}.sysu.edu.cn

ABSTRACT

In order to improve the accuracy of fingerprint-based localization, one may fuse step counter measurement with location estimation. Previous works on this often require a pre-calibrating the step counter with training sequence or explicit user input, which is inconvenient for practical deployment. Some assume conditional independence on successive sensor readings, which achieves unsatisfactory accuracy in complex and noisy environment. Some other works need a calibration process for RSSI measurement consistency if different devices are used for offline fingerprint collection and online location query.

We propose SLAC, a fingerprint positioning framework which simultaneously localizes the target and calibrates the system. SLAC is calibration-free, and works transparently for heterogeneous devices and users. It is based on a novel formulation embedded with a specialized particle filter, where location estimations, wireless signals and user motion are *jointly* optimized with resultant consistent and correct model parameters. Extensive experimental trials at HKUST campus and Hong Kong International Airport further confirm that SLAC accommodates device heterogeneity, and achieves significantly lower errors compared with other state-of-the-art algorithms.

ACM Classification Keywords

C.2.m. Computer Systems Organization:Computer Communication Network: Miscellaneous

Author Keywords

Indoor localization; joint optimization; device RSSI dependency; step counter calibration; fingerprinting; fusion.

INTRODUCTION

Indoor Location-Based Service (LBS) has attracted wide attention in recent years due to its social and commercial values, with total revenue predicted to worth 10 billion US dollars by 2020 [1]. The service quality of indoor LBS largely depends on the localization accuracy of users [25]. Among all the current indoor localization techniques, Wi-Fi fingerprinting emerges as a promising one, as it does not assume line-of-sight

measurement and is adaptive to complex indoor environment without deployment of extra infrastructure [24, 36].

Fingerprint-based indoor localization is usually conducted in two phases: offline phase (survey) and online phase (query) [16, 24, 34]. In the offline phase, a site survey is conducted to collect the vectors of received signal strength indicator (RSSI) from access points (APs) at reference points (RPs) with known locations. In the offline phase, given a query with RSSI measurement, a target (in this paper, we use "user", "client" and "target" interchangeably) obtains her or his location with the closely-matched signals in the database.

With the advance in smartphone sensors of accelerometers and gyroscopes [14], fusing motion with wireless fingerprint has been recently studied to improve localization accuracy [27, 41, 47]. While fusing step counter and fingerprinting has shown to be promising, many practical issues remain to be addressed. Among them, a critical one is system calibration for both devices and users. *Device heterogeneity* arises when different devices are used to measure the same wireless signal [23]. As their RSSI may not agree with each other, the RSSI difference needs to be calibrated, traditionally by offline training. *User heterogeneity* arises when the motion sensors for different users need to be calibrated with different parameters in system operation. In step counter, user stride length is different for different users, and is related to some stride frequency model [53]. Traditional localization techniques based on Wi-Fi fingerprint and step counter fusion often require explicit input of stride model parameters, or tedious intrusive training offline.

We show in Figure 1(a) the traditional localization approach fusing step counter measurement and Wi-Fi fingerprints. The device first needs to be calibrated to align the RSSI measurement with the fingerprint. The step counter measures the change in user motion [14] with step frequency and count as output. Based on a step length model, user displacement may be estimated by summing the stride length over all the steps. Through some probabilistic inference [9] between wireless signals and walking displacement [10, 33], the system estimates the current user location. It is clear that external parameter calibrations are needed in both device dependency model and step length model.

Observe that when a user walks, her/his spatial location, wireless signals received (as measured by the device), and displacement (as measured by the step counter as stride model) are correlated. Specifically, distance between location estimations

Figure 1. Comparison between traditional and proposed schemes: (a) traditional approach; (b) joint localization and calibration approach.

Figure 2. System work flow of the generic framework in SLAC.

should be *consistent* with the measured walking displacement. Such correlation can be utilized to calculate the target location given the stored fingerprint map, leading to higher accuracy. Especially in indoor open space like spacious airports or stations, it is also important to constrain the target estimation using above correlations, as it is often difficult to characterize the degree of freedom for user mobility there [18, 41]. The estimated target locations can be in turn used to calibrate model parameters for both device and user heterogeneities.

Armed with the above observations, we consider simultaneously localizing the target and calibrating the localization system transparently without user input, i.e., a calibration-free approach. As shown in Figure 1(b), the correlations between signals and walking displacements are jointly considered in our fusion algorithm. The consistency requirement between spatial measures (namely RF signals received at the users) and temporal measures (namely step frequency and counts reported by the step counter) is used as constraint to self-calibrate the parameters for the device dependency and step length models. Using such approach, signal noise from each sensor can be mitigated, while the system can achieve high localization accuracy and calibration without explicit user participation.

We propose SLAC, a calibration-free framework which conducts **s**imultaneous **l**ocalization **a**nd **c**alibration fusing step counter and fingerprints. Figure 2 shows the work flow of S-LAC. In the offline phase, SLAC is initiated with a site survey, storing the Wi-Fi fingerprints of reference points (RPs) into the database. In the online phase, the target (client) collects Wi-Fi RSSI vectors and measures user walking steps. The server then fuses a step length model and stride frequency with the RSSI signal received, and solves a joint optimization problem to localize the user with the simultaneous calibration of the step length model. Given the estimated locations, the system utilizes particle filter to calibrate the RSSI difference due to device heterogeneity. It is clear that such self-calibration is transparent to the user.

The unique and salient features of SLAC are as follows:

- *Simultaneous Localization and Calibration:* SLAC is a novel framework which achieves indoor localization and transparent system calibration simultaneously. SLAC learns
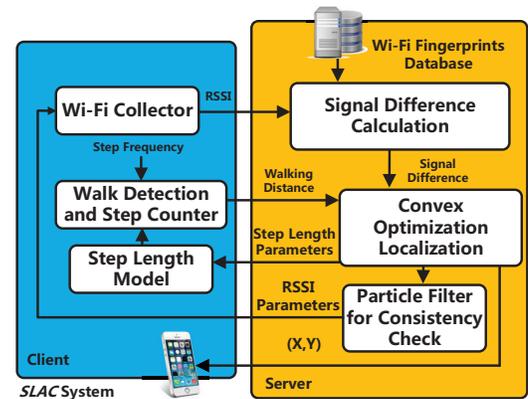
parameters in user step model, and meanwhile calibrates RSSI measurements due to heterogeneous devices. To our best knowledge, SLAC is *the first generic framework* which can jointly and transparently achieve accurate location estimations, calibrate device dependency and adapt to user motion heterogeneity without explicit user participation.

- *Fusing Joint Optimization with Particle-Filter Learning:* We formulate a novel optimization problem fusing particle filter. In such formulation, SLAC leverages the spatial-temporal correlation between target locations, RSSI signals and step counts. It jointly considers the correlation between location estimations and different sensors in a single optimization. By solving a convex optimization problem, we accurately estimate the location of the walking target. The temporal information of user position is meanwhile fed to a specialized particle filter to check the consistency, as inspired in Figure 1(b), and infer the corresponding system parameters.

- *Consideration of Sensor Measurement Uncertainty:* SLAC advances from previous works by jointly considering measurement uncertainty in wireless signals and distances. We consider the randomness of fingerprints in our optimization formulation to mitigate noise influence. Furthermore, we consider distance estimation uncertainty of motion sensors. Our particle filter utilizes the above uncertainty to check the convergence of learning. Therefore, we can achieve high estimation robustness under noisy environments.

We have implemented SLAC on the Android platform and conducted large-scale testbed experiments in the Hong Kong International Airport (HKIA) and The Hong Kong University of Science and Technology (HKUST). Experimental results show that our scheme outperforms other approaches in localization accuracy, with transparent calibration of step counter (user heterogeneity) and RSSI signals (device heterogeneity). Note that though our discussion is mainly on Wi-Fi fingerprints, SLAC is general enough to be applicable to other survey-based or fingerprint signals such as RFID [12], visible light [46], channel state information (CSI) [42, 48] or magnetic field [45].

The rest of this paper is organized as follows. We first discuss the preliminaries in SLAC system. Then we describe the core

algorithm of SLAC. After that, we present its experimental results in two sites. Finally, we summarize our work.

RELATED WORK

We briefly review related work as follows. Due to ease of deployment [36], Wi-Fi fingerprinting techniques, including RADAR [3], Horus [49], WiGEM [11], Sectjunction [15] and Compressive Sensing [7], have been widely studied in recent years. The above works are based on solely Wi-Fi fingerprinting. We, on the other hand, fuse user motion into fingerprints to achieve much better accuracy.

To fuse step counter measurement and Wi-Fi fingerprint, recent works like Markov model [31, 33, 39], signal pattern matching [32], conditional random field [43] and particle filter [10, 18, 35] have been studied for indoor localization [47]. Wi-Fi SLAM [8] also utilizes robot odometer to fuse accurate distance with wireless signals. However, these works usually rely on specific probabilistic assumption between different noisy sensors and may work the best under narrow office environment. Our scheme, in contrast, jointly utilizes wireless signals and motion sensors in a single optimization, and thus can achieve higher accuracy and robustness under noisy measurements. Furthermore, our framework, based on joint location mapping and learning, is adaptive to different environments, including large open space (like the airport) or narrow corridors (like the office building).

In addition, the works based on step counter and Wi-Fi fusion above often consider a pre-calibrated step counter for displacement estimation [38]. Some offline stride calibration methods on step counter have been proposed. However, they either require offline calibration [18, 22], or deploy external sensor infrastructures for walking distance estimation [37, 51]. Our work, in contrast, adaptively fuses available wireless fingerprints for online step counter calibration without explicit user input, and hence can be integrated with existing smartphone-based indoor localization systems [3, 13].

Device dependency in wireless signal measurement has been studied in recent years [6, 21, 26]. The work in [21] considers a linear model to calibrate the RSSI signals offline. Online signal adaptation [11, 23, 26] has been recently studied to facilitate the calibration. However, they are solely based on the measured RSSI and have not fully taken advantage of the correlation between fingerprint signals, locations and motion information. To our best knowledge, SLAC is the first framework to utilize step counter fusion to jointly calibrate the device RSSI, achieving much higher adaptability.

PRELIMINARIES OF SLAC

In this section, we present the preliminaries of SLAC. We first discuss the RF signals in the context of Wi-Fi fingerprints and the device dependency in RSSI. Then we briefly describe the motion estimations and the heterogeneity in user step length profile.

Fingerprint RSSI Measurement

In the offline phase of fingerprint-based localization, a site survey is conducted on overall Q reference points (RPs). Let $\mathbf{r}_q$ be the 2-D position of RP q, and $\mathbf{R} = [\mathbf{r}_1, \mathbf{r}_2, \ldots, \mathbf{r}_Q]$ be a

Table 1. Major symbols used in SLAC.

Notation	Definition
$\widehat{\mathbf{x}}_m^p$	Estimated 2-D coordinate of the target user
δ_{mn}	Distance between temporal targets m and n (m)
S_c	Step length at step c (m)
f_c	Step frequency at step c (Hz)
$\mathbf{r}_q$	2-D coordinate of reference point (RP) q
Q	Number of RPs in fingerprint database
ω_{mq}^p	Weight of RP q in set p in estimating target m
L	Number of APs
ψ_q^l	RSSI received at RP q from AP l (dBm)
ϕ_m^l	RSSI received at target m from AP l (dBm)
$\boldsymbol{\psi}_q$	RSSI vector received at RP q
$\boldsymbol{\phi}_m$	RSSI vector received at target m
$\bar{\psi}_q^l$	RSSI for AP l at RP q (dBm)
T_q^l	Number of RSSI measurements at q for AP l
σ_q^l	RSSI standard deviation at RP q for AP l (dB)
θ^p	Weight of particle p
$[k_p, b_p]$	Parameters in linear RSSI model between stored and online devices for particle p
$[\alpha, \beta]$	Parameters in linear step length model
P	Number of particles for consistency check

2-by-Q matrix indicating the RP positions. Let $\mathcal{L}$ be the set of L Wi-Fi access points (APs) that cover the site.

At each RP, multiple Wi-Fi RSSI samples are collected to reduce measurement uncertainty. Denote the RSSI at RP q from AP l at time t as $\psi_q^l(t)$, $1 \le t \le T_q^l$ $\left(T_q^l > 1\right)$, with T_q^l being the total number of samples collected. Let $\bar{\psi}_q^l$ be the average RSS reading over time domain for AP l, $l \in \mathcal{L}$, at RP q, and $\left(\sigma_q^l\right)^2$ be the unbiased estimate of variance in RSS time samples for AP l at RP q. Then for each RP, the mean RSSI is computed as

$$\bar{\psi}_q^l = \frac{1}{T_q^l}\left(\sum_{t=1}^{T_q^l} \psi_q^l(t)\right), \tag{1}$$

and the corresponding RSSI variance is given by

$$\left(\sigma_q^l\right)^2 = \frac{1}{T_q^l - 1}\left(\sum_{t=1}^{T_q^l} \left(\psi_q^l(t) - \bar{\psi}_q^l\right)^2\right). \tag{2}$$

Then the Wi-Fi RSSI vector at RP q is

$$\boldsymbol{\psi}_q = \left[\bar{\psi}_q^1, \bar{\psi}_q^2, \ldots, \bar{\psi}_q^L\right], q \in \{1, 2, \ldots, Q\}. \tag{3}$$

In the online phase, the device continuously measures the Wi-Fi RSSI vectors as the user walks. These vectors form the *temporal targets* with locations to be estimated. We consider a sliding window of M temporal targets for joint localization, and the M-th one is the latest measurement. Let ϕ_m^l be the RSSI value at target m ($1 \le m \le M$) from Wi-Fi AP l, $l \in \mathcal{L}$. Similar to RP RSSI vector, we define the sampled RSSI vector
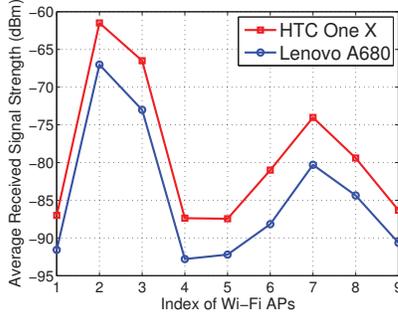
Figure 3. RSSI vectors collected from HTC One X and Lenovo A680.

at target point m as

$$\boldsymbol{\phi}_m = \left[\phi_m^1, \phi_m^2, \ldots, \phi_m^L\right]. \tag{4}$$

By definition, if an RP or target cannot detect signals from AP l, $\bar{\psi}_q^l = 0$ and $\sigma_q^l = 0$ (or $\phi_m^l = 0$).

Device Dependency in RSSI Measurement

Due to the difference in Wi-Fi network interfaces, for the same RF signal, different types of smartphones may have different measurement values [26]. To illustrate this, we conduct an experiment and collect $1,000$ RSSI samples using HTC One X and Lenovo A680, respectively. Figure 3 shows the linear shift between the signals of the two smartphones.

In order to reduce such device dependency, there have been a lot of models used for calibration [11, 23]. In this paper, for concreteness we implement a linear signal model to adjust the device heterogeneity. Given an RSSI ϕ_m^l (in dBm) at target m, we find the corresponding *device parameters*, denoted as k ($k > 0$) and b, i.e.,

$$\widetilde{\phi}_m^l = k\phi_m^l + b. \tag{5}$$

The calibrated signal value $\widetilde{\phi}_m^l$ is then utilized for the signal vector comparison. In our formulation, we are to find the tuple $[k, b]$ which fits the device difference. Though our paper uses a linear model in device calibration for concreteness, SLAC may be compatible to other more advanced models, e.g. [28].

Walk Detection and Step Counting

Besides RF signals, the client also measures walking information through the inertial sensors on smartphones. A step counter has two modules: walking detection and step counting [5]. Walk detection classifies the current state of the target. If a user is identified as moving, the step counting measures her/his displacement with step counts and stride length [16].

Denote the magnitude of linear acceleration and rate of rotation as a_t (m/s^2) and ρ_t (rad/s) respectively. Given a sliding window of $\mathcal{W}$ measured values, we consider the average magnitude of linear acceleration, denoted as h_a, and the standard deviation of angular velocity, denoted as h_ρ [5], for motion detection:

$$h_a = \frac{\sum_{t=1}^{\mathcal{W}} a_t}{\mathcal{W}}, \ h_\rho = \frac{1}{\mathcal{W}} \sum_{t=1}^{\mathcal{W}} \left(\rho_t - \frac{\sum_{t=1}^{\mathcal{W}} \rho_t}{\mathcal{W}}\right)^2. \tag{6}$$

If h_a and h_ρ are below certain thresholds, then the user is classified as static [5]. Otherwise, the user is identified as

moving and the step counter measures the walking steps. We implement the step counting algorithm in [22, 30]. A repetitive step pattern in the accelerometer is discovered through the normalized autocorrelation [30].

User Heterogeneity in Step Length Measurement

Based on step counting, we estimate the walking distance by multiplying number of steps with stride length. The step length is estimated based on the following model. Denote the step length at the c-th step as $\mathcal{S}_c$ (m) and the corresponding step frequency as f_c (Hz). The linear relationship between them is given by

$$\mathcal{S}_c = \alpha f_c + \beta, \tag{7}$$

where the *step parameters*, α ($\alpha > 0$) and β, are user dependent [37]. Then given C_{mn} steps between two locations (temporal targets) m and n with Wi-Fi measurements, the walking distance is given by $\delta_{mn} = \sum_{c=1}^{C_{mn}} \mathcal{S}_c$.

For ease of prototyping, we implement the linear model for step length estimation. Note that our calibration is independent of step length model and can be generic enough to apply in more sophisticated ones [29, 50]. To summarize, our goal in SLAC is to locate the target user given sets of signals, $\{\boldsymbol{\psi}_q\}$ and $\{\boldsymbol{\phi}_m\}$, while calibrating $[k, b]$ in RSSI and $[\alpha, \beta]$ in user profile transparently without explicit user input.

SIMULTANEOUS LOCALIZATION & SELF-CALIBRATION

Given the above preliminaries, we present in this section how we formulate a novel joint optimization and specialized particle filter in SLAC. Candidate parameters in device RSSI mapping are first generated. Then the closeness between target signals and fingerprints are calculated. Given distance measurements, a proposed joint optimization finds the target locations and consistent parameters in step length model. Particle filter simultaneously adjusts RSSI model parameters to mitigate the influence of device dependency.

Wireless Signal Difference

To retrieve the correct parameters in Equation (5), we formulate a specialized particle filter [2] for device calibration. Potential model parameters are generated and filtered during the joint optimization. As we are to use the calibrated signals for localization at the same time, we first present in the following how to compare the signal vectors to represent the closeness with the fingerprint map.

In the initialization stage, we generate P sets of device parameter tuples, denoted as $\{[k_p, b_p]\}$, which are later used to generate P candidate locations for each temporal target. A uniform initial sampling is first conducted in the potential interval of

$$k_{min} \le k_p^0 \le k_{max}, \ b_{min} \le b_p^0 \le b_{max}, \tag{8}$$

where the initial interval can be obtained through empirical studies [53]. Above parameter candidates are used for signal comparison and joint location estimation. SLAC will then estimate the most suitable $[k_p, b_p]$ for the device calibration.

In comparing the signal vectors, we jointly consider device heterogeneity in Equation (5) and measurement uncertainty

in Equation (2) [17]. Let $\mathbf{S}_{mq}$ be the shared APs between the temporal target m and RP q $(0 < |\mathbf{S}_{mq}| \leq L)$. Given a target's Wi-Fi RSSI ϕ_m^l (constant) from AP $l \in \mathbf{S}_{mq}$ and parameter candidate $[k_p, b_p]$, the expected signal difference between RP q and the target RSSI in AP l is defined as:

$$\Delta_p^l(\boldsymbol{\phi}_m, \boldsymbol{\psi}_q) \triangleq \mathrm{E}\left(\left(\widetilde{\phi}_m^l - \psi_q^l\right)^2\right)$$

$$= \mathrm{E}\left(\left(\widetilde{\phi}_m^l\right)^2 - 2\phi_m^l\psi_q^l + \left(\psi_q^l\right)^2\right)$$

$$= \left(\widetilde{\phi}_m^l\right)^2 - 2\phi_m^l\mathrm{E}\left(\psi_q^l\right) + \mathrm{E}\left(\left(\psi_q^l\right)^2\right)$$

$$= \left(\widetilde{\phi}_m^l\right)^2 - 2\phi_m^l\mathrm{E}\left(\psi_q^l\right) + \mathrm{E}^2\left(\psi_q^l\right) + \left(\sigma_q^l\right)^2$$

$$= \left(k_p\phi_m^l + b_p - \bar{\psi}_q^l\right)^2 + \left(\sigma_q^l\right)^2, \qquad (9)$$

where, by definition, $\Delta_p^l(\boldsymbol{\phi}_m, \boldsymbol{\psi}_q) = 0$, if AP l is not detected at either or both sides. Thus, the overall expected signal difference between $\boldsymbol{\phi}_m$ and $\boldsymbol{\psi}_q$ for candidate (particle) p is given by

$$\Gamma_p(\boldsymbol{\phi}_m, \boldsymbol{\psi}_q) \triangleq \frac{1}{|\mathbf{S}_{mq}|} \sum_{l=1}^{|\mathbf{S}_{mq}|} \Delta_p^l(\boldsymbol{\phi}_m, \boldsymbol{\psi}_q). \qquad (10)$$

If $|\mathbf{S}_{mq}| = 0$, RP q is not considered in estimating target m.

Location Estimation Problem and Walking Distance Constraint

For each candidate $[k_p, b_p]$, we estimate the target's potential location using Equation (10) and the measured distance constraints from motion sensors in Equation (7).

Given a tuple $[k_p, b_p]$, let $\mathbf{V}^p = \{1, 2, \ldots, M\}$ be the time index of each temporal target in the sliding window, and $\widehat{\mathbf{x}}_m^p, m \in \mathbf{V}^p$ be the location for each of them to be estimated. RPs in $\mathbf{R}$ are used to locate these target positions. For a candidate p, let ω_{mq}^p be the weight assigned to RP q when locating target m, and we have

$$\widehat{\mathbf{x}}_m^p = \sum_{q=1}^{Q} \omega_{mq}^p \mathbf{r}_q, \qquad (11)$$

where the weights $\omega_{mq}^p, \forall m$, are constrained by

$$\sum_{q=1}^{Q} \omega_{mq}^p = 1, \quad \omega_{mq}^p \geq 0, \quad \forall q \in \{1, 2, \ldots, Q\}. \qquad (12)$$

As the target is more likely be between the RPs, we assign additional constraint over ω_{mq}^p as

$$\omega_{mq}^p \leq \lambda^p. \qquad (13)$$

Here constraint λ^p is given by

$$\lambda^p = \frac{\max \Gamma_p(\boldsymbol{\phi}_m, \boldsymbol{\psi}_q)}{\sum_{q=1}^{N} \Gamma_p(\boldsymbol{\phi}_m, \boldsymbol{\psi}_q)}, \qquad (14)$$

where N is the number of signal differences used for averaging ($N = 10$ in our experiment).

Localization & Self-calibration Using Joint Optimization

In such localization process, we would like to basically search against the fingerprint map to find the RPs which both minimize the signal differences and satisfy the sequential distance measurements. In order to efficiently solve this problem, we formulate a joint optimization. Based on Equations (10) and (15), we first present as follows the objective function of S-LAC.

Recall that the measured distance between $\widehat{\mathbf{x}}_m^p$ and $\widehat{\mathbf{x}}_n^p$ as δ_{mn} for each two sequential targets m, n. To jointly localize all the temporal targets in $\mathbf{V}^p$, we would like to find a set of locations $\widehat{\mathbf{x}}_1^p, \widehat{\mathbf{x}}_2^p, \ldots, \widehat{\mathbf{x}}_M^p \in \mathbb{R}^2$ in the survey site in order to minimize

$$\sum_{m=2}^{M} \left(\|\widehat{\mathbf{x}}_m^p - \widehat{\mathbf{x}}_n^p\|_2 - \delta_{mn}\right)^2, n = m - 1, \qquad (15)$$

All the temporal targets under different device RSSI parameters $\{[k_p, b_p]\}$ are jointly considered in the objective function. Let $[\alpha_{min}, \alpha_{max}]$ and $[\beta_{min}, \beta_{max}]$ be the range for step parameter calibration. For simultaneous calibration, we are to find the weights and $[\alpha, \beta]$, which jointly minimize difference between measured distances and relative positions of all estimated targets, i.e.,

$$\underset{\{\omega_{mq}^p\}, [\alpha, \beta]}{\arg\min} \sum_{p=1}^{P} \sum_{m=2}^{M} \left(\|\widehat{\mathbf{x}}_m^p - \widehat{\mathbf{x}}_n^p\|_2 - \delta_{mn}\right)^2, \qquad (16)$$

where $n = m - 1$. In other words, this objective function requires the location estimations to consistently satisfy their sequentially measured distances. Step parameters in Equation (7) are therefore retrieved through the above consistency.

Due to changes in heading direction, holding gestures and other factors [44], readings from motion sensors often carry noise. In order to be robust towards such measurement fluctuation, we further implement the Berhu loss function [4] to replace the squared errors. Berhu loss function has been widely implemented for robust fitting [4], and is defined as follows:

DEFINITION 1. *Given the difference z, the corresponding Berhu loss, denoted as $\mathcal{B}(z)$, is*

$$\mathcal{B}(z) \triangleq \begin{cases} |z| & |z| \leq T, \\ \frac{z^2 + T^2}{2T} & |z| > T. \end{cases} \qquad (17)$$

T is a tunable parameter which determines the penalty range.

Berhu loss function means that when the difference between $\|\widehat{\mathbf{x}}_m^p - \widehat{\mathbf{x}}_n^p\|_2$ and δ_{mn} is small, the penalty grows slowly so it can tolerate small measurement fluctuation. If the difference is large, Berhu loss assigns more penalty. Then the objective function can be rewritten as

$$\underset{\{\omega_{mq}^p\}, [\alpha, \beta]}{\arg\min} \sum_{p=1}^{P} \sum_{m=2}^{M} \mathcal{B}\left(\|\widehat{\mathbf{x}}_m^p - \widehat{\mathbf{x}}_n^p\|_2 - \delta_{mn}\right), \qquad (18)$$

where $\forall n = m - 1$.

In order to simultaneously minimize the signal difference for location estimations, we utilize an upper bound constraint to

reduce the difference between target RSSI signals and fingerprints [4]. In other words, in the joint optimization, RPs with larger signal difference are assigned with lower weights ω_{mq}^p. Denote the upper bound constraint for estimation using parameter set q as γ^p, which is given by

$$\sum_{m=1}^{M}\left(\sum_{q=1}^{Q}\Gamma_p(\boldsymbol{\phi}_m,\boldsymbol{\psi}_q)\omega_{mq}^p\right) \leq \gamma^p, \qquad (19)$$

where $\gamma^p = g \sum_{m=1}^{M} \min \Gamma_p(\boldsymbol{\phi}_m,\boldsymbol{\psi}_q)$ and g is a tunable parameter. In this way, the correlation of mapping between the measured RSSIs and stored fingerprints is fused into our formulation to provide absolute target positions.

To summarize, we are to find P candidate locations $\widehat{\mathbf{x}}_m^p$ and $[\alpha,\beta]$ such that the overall walking distance differences are jointly minimized given signal difference constraints, i.e.,

$$\begin{aligned} &\text{Objective: Equation (18),} \\ &\text{subject to: Equations (11), (12), (13) and (19).} \end{aligned} \qquad (20)$$

Particle Filter for Calibration Consistency
The above formulation have generated $[\alpha,\beta]$, candidates $\{[k_p,b_p]\}$ and corresponding locations $\{\widehat{\mathbf{x}}_m^p\}$. Given above, we propose below a specialized particle filter for parameter calibration, i.e., to find the most suitable $[k_p,b_p]$ which are consistent with estimated locations. Different from previous works using particle filter for localization fusion [40], our work utilizes it only for parameter learning with smaller degree of freedom and cost of computation.

We calculate the distance between neighboring $\{\widehat{\mathbf{x}}_m^p\}$ and evaluate their consistency with mutual distances obtained from step counter. More specifically, given $[k_p,b_p]$, $\forall p$, denote the distance between $\widehat{\mathbf{x}}_m^p$ and $\widehat{\mathbf{x}}_n^p$ as

$$d_{mn}^p = \|\widehat{\mathbf{x}}_m^p - \widehat{\mathbf{x}}_n^p\|, n = m-1, \forall m \in \{2,\dots,M\}. \qquad (21)$$

Then, given measured walking distance δ_{mn} from step counter, we calculate the weight θ_p of each particle based on the consistency between δ_{mn} and d_{mn}^p as

$$\theta_p = \frac{1}{\sqrt{2\pi}\sigma_w} \exp\left(-\frac{\left(\sum_{m=2}^{M}\delta_{mn} - \sum_{m=2}^{M}d_{mn}^p\right)^2}{2\sigma_w^2}\right), \qquad (22)$$

where σ_w is the sensitivity of the weight. Hence θ_p represents the consistency between δ_{mn} and d_{mn}^p. In other words, those parameters which match the measured distance δ_{mn} get large weights. Each weight will then be normalized, i.e.,

$$\theta_p \leftarrow \frac{\theta_p}{\sum_{p=1}^{P} \theta_p}. \qquad (23)$$

Then the particles get resampled according to θ_p [2, 45]. As the user collects multiple Wi-Fi measurements during walking, $[k_p,b_p]$ get calibrated. The weights of resampled parameters will be normalized, and the final $[\hat{k},\hat{b}]$ are given by

$$\hat{k} = \sum_{p=1}^{P} \theta_p k_p, \quad \hat{b} = \sum_{p=1}^{P} \theta_p b_p. \qquad (24)$$

Through resampling, the parameters with low consistency will be filtered due to the low weights. The estimated location of the M-th target (i.e., the current position) is given by the weighted average of the locations generated from particles,

$$\widehat{\mathbf{x}}_M = \sum_{p=1}^{P} \theta_p \widehat{\mathbf{x}}_M^p. \qquad (25)$$

Convergence Criterion and Complexity Analysis
If the estimations using the above parameters $[k_p,b_p]$ converge, we can simply use $[\hat{k},\hat{b}]$ (Equation (24)) for localization. Therefore, we measure the uncertainty of walking displacement as the convergence criterion for SLAC. Specifically, given f_c, variance of estimated step length at time c is

$$\begin{aligned} Var(S_c) &= Var(\alpha f_c + \beta) \\ &= \alpha^2 Var(f_c) + \beta^2, \end{aligned} \qquad (26)$$

where $Var(f_c)$ is the variance of step frequency in the sliding window (M temporal targets). For the two sequentially estimated locations m and n ($n = m-1$), given C_{mn} values of measured step frequency, variance of δ_{mn} is given by

$$Var(\delta_{mn}) = Var\left(\sum_{c=1}^{C_{mn}} S_c\right) = \sum_{c=1}^{C_{mn}} Var(S_c). \qquad (27)$$

SLAC checks the convergence after each time of joint calibration. Specifically, for the M-th temporal target, we define the dispersiveness of candidate locations as the average distance between estimated particles $\widehat{\mathbf{x}}_M^p$ and their mean $\widehat{\mathbf{x}}_M$, i.e.,

$$\xi \triangleq \frac{1}{P} \sum_{p=1}^{P} \|\widehat{\mathbf{x}}_M^p - \widehat{\mathbf{x}}_M\|. \qquad (28)$$

Given the calculated δ_{mn} (distance between current and previous positions), if ξ is smaller than a certain threshold, i.e.,

$$\xi \leq \eta \sqrt{Var(\delta_{mn})}, \qquad (29)$$

where η indicates the confidence interval, we can conclude that the self calibration converges. The later indoor localization is conducted based on $[\hat{k},\hat{b}]$ and calibrated $[\alpha,\beta]$ (i.e., $P = 1$ and $[\alpha,\beta]$ in the joint optimization becomes constant).

We briefly describe the computational complexity here. Given Q RPs and L APs, the complexity of signal difference calculation is $O(QL)$. Usually the number of temporal targets M (size of sliding window) is small. Then the complexity of solving convex optimization for each single user is $O(PQ^3M^3)$ [4] on the server side. Further computation reduction can be conducted by AP filtering and RP cluster mapping [7] to reduce the number of APs and RPs. By filtering those APs which do not differentiate the RPs well (reducing L), we can reduce the time in signal difference calculation [7, 15]. The target location can be first mapped to a small region (like RP cluster [7]) of the floor plan. Then Q is significantly reduced and computation of SLAC decreases. After calibration converges, $P = 1$, $[\alpha,\beta]$ are fixed and the online localization complexity is small. In future work, further increasing scalability for large-scale deployment will be investigated.

Algorithm 1: SLAC: Simultaneous Localization & Calibration.

Input: **F**: set of step frequency in the sliding window.
  P: number of particles for consistency check.
  $\{\phi_m\}$ and $\{\psi_q\}$: measured RSSIs at target and RPs.
Output: Ω: set of parameters for walking model.
  $\{\widehat{\mathbf{x}}\}$: estimated locations of the target.

1 $\Omega \leftarrow \{\}./\ast$ `Initialization` $\ast/$
2 **if** *NoParticles* **then**
3   **for** $p \leftarrow 1$ *to* P **do**
4      $[k_p, b_p] \leftarrow \text{RandSam}([k_{min}, k_{max}], [b_{min}, b_{max}]);$
5   Add $[k_p, b_p]$ into Ω;
6   **end**
7 **end**
   $/\ast$ `Joint localization and calibration` $\ast/$
8 Localization based on Formulation (20).
9 **for** $m \leftarrow 2$ *to* M **do**
10   $n \leftarrow m - 1;\ \delta_{mn}^p \leftarrow 0;$
11   **for** *each* $f_c \in \mathbf{F}$ **do**
12     $\delta_{mn}^p \leftarrow \delta_{mn}^p + (\alpha f_c + \beta);$
13   **end**
14 **end**
15 $\delta^p = \sum_{m=2}^{M} \delta_{mn}^p; /\ast$ `Measured walking dist` $\ast/$
16 **for** $p \leftarrow 1$ *to* P **do**
17   $d^p \leftarrow 0;$
     $/\ast$ `Dist between estimated locations` $\ast/$
18   **for** $m \leftarrow 2$ *to* M **do**
19     $d^p \leftarrow d^p + \|\widehat{\mathbf{x}}_m^p - \widehat{\mathbf{x}}_{m-1}^p\|_2;$
20   **end**
21   $\theta_p \leftarrow \exp\left(-(d^p - \delta^p)^2 / \left(2\sigma_w^2\right)\right) / \left(\sqrt{2\pi}\sigma_w\right);$
     $/\ast$ `Particle weight recalculation` $\ast/$
22 **end**
    $/\ast$ `Resampling of particles` $\ast/$
23 **for** $p \leftarrow 1$ *to* P **do**
24   $\{[k_p, b_p], \theta_p\} \leftarrow Resample\,(\Omega);$
25 **end**
26 *NormalizeWeight*$(\{\theta_p\}); /\ast$ `Normalization` $\ast/$
27 $\widehat{\mathbf{x}}_M \leftarrow \sum_{p=1}^{P} \theta_p \widehat{\mathbf{x}}_M^p; /\ast$ `Final estimation` $\ast/$

To summarize, the flow of SLAC is presented in Algorithm 1. Through initial random sampling, we generate multiple sets of parameters as input in the RSSI model in Equation (5) (Lines 2 to 6). Based on these parameters, we conduct the localization with Formulation (20) (Lines 8 to 15). As each parameter set corresponds to a location estimation, we filter the inconsistent parameters and resample the others using the difference in their mutual distances of Equation (22) (Lines 16 to 24).

ILLUSTRATIVE EXPERIMENTAL RESULTS

We evaluate the SLAC framework prototype in part of the Hong Kong International Airport (HKIA) (Figure 4) and our university atrium at HKUST (Figure 5). As shown in the photos, these survey sites include wall partitions and large open space. Figure 6 and Figure 7 show their survey floor plans, respectively. In the following, we will present the experimen-

Figure 4. Survey site of airport boarding area at HKIA.

Figure 5. Survey site of campus atrium at HKUST.

tal settings and comparison schemes, followed by illustrative results in these two sites.

Experimental Settings and Comparison Schemes

We have implemented SLAC on Android platforms. In HKIA, we collect 350 RPs in overall $10,000\ \text{m}^2$ area. Similarly, in our HKUST campus, we collect 200 RPs in overall $4,000\ \text{m}^2$ area. The site survey is conducted in each site for over a day. At each RP, we take totally 80 Wi-Fi RSSI vectors using HTC One X (each sample takes 1 second). A quarter of these samples are collected when we are facing north, south, west and east, respectively. The grid size of site survey is 5 m.

During testing phase, the users collect the testing data (RSSI and INS) during walking, and explicitly record the ground truth when they pass by landmarks (like pillars, windows or doors). Time stamps of the readings are also recorded during testing. Smartphones are held in front of the users (like internet browsing and map reading) during walking, as it is the traditional gesture for indoor navigation service. (Note that other holding gestures, including being in pockets or shaking, can be easily filtered through some classification [20, 44, 52], as they may correspond to conditions when users may not need real-time user navigation service in real system deployment. Further classification will be considered in the future work.)

We compare the performance of SLAC with the following state-of-the-art localization and fusion schemes:

- *Fingerprint-based Localization* (FL), the classical algorithm [3, 13] which evaluates Euclidean distance of each target RSSI vector with the fingerprints at RPs and finds the top K nearest neighbors in signal space for location estimation.

- *Maximum-Likelihood-based Localization* (MLL), a recent scheme which considers sequential probability along the walking trajectory [31]. Assuming conditional independence between sequential sensor measurements, it calculates the product of probability obtained through Wi-Fi and motion estimation [31, 33]. Then it finds the location with the maximum likelihood [43] as the target position.

- *Particle-Filter-based Localization* (PFL), a typical fusion algorithm [10, 18, 30] based on particle filter, which fuses walking distance and Wi-Fi fingerprints. The weights of particles are updated according to Wi-Fi location estimation and walking path [10]. Then these particles are resampled according to their weights and map constraints [30].
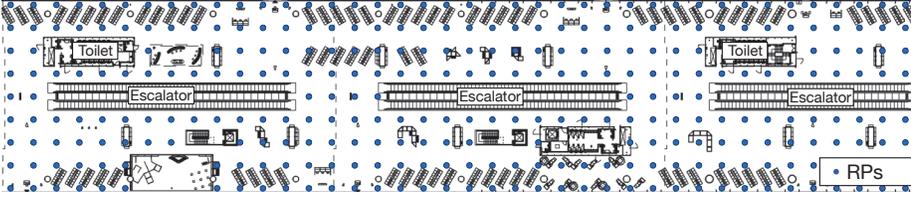
Figure 6. Floor plan of the boarding area in HKIA. The site survey density is 5 m.
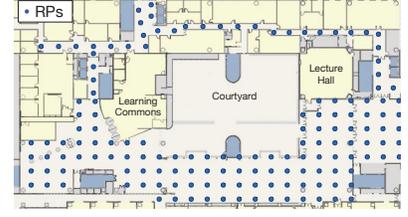
Figure 7. Floor plan of HKUST atrium.
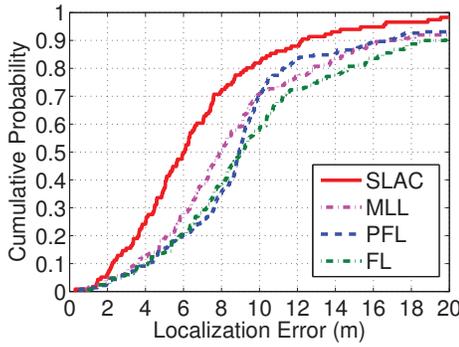
Figure 8. Performance of SLAC after calibration convergence (airport).
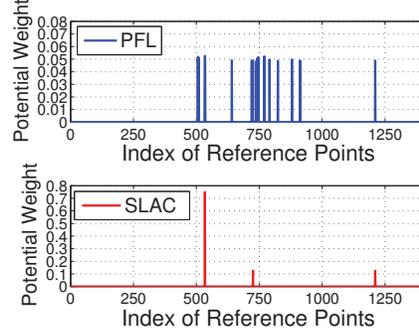
Figure 9. Reducing dispersed nearest neighbors through joint optimization (airport).
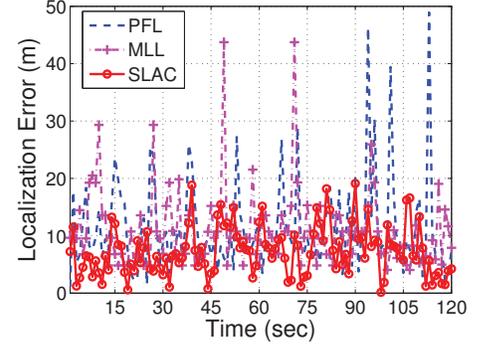
Figure 10. Localization performance over time (airport).
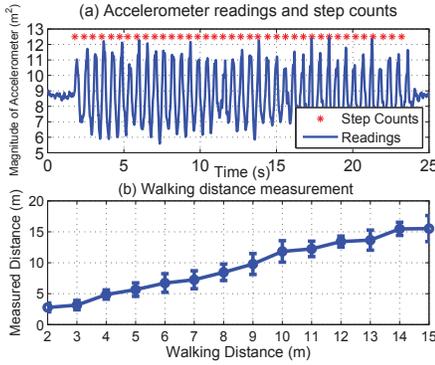
Figure 11. (a) Step counter readings in SLAC; (b) accuracy at different walking distances.
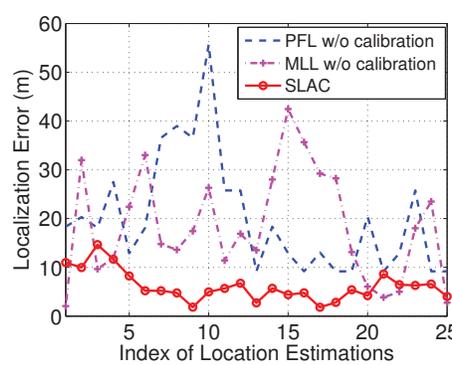
Figure 12. Localization error convergence of SLAC in the initial learning process (airport).
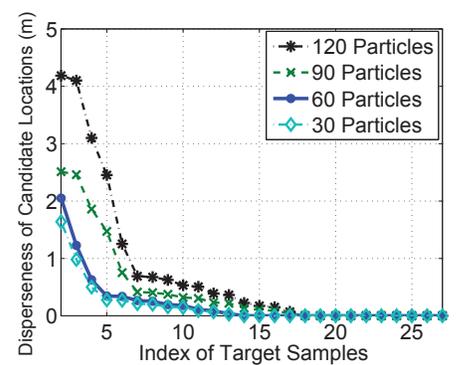
Figure 13. Convergence of location estimation dispersiveness during self calibration (airport).

For approaching RSSI device dependency, we also compare SLAC with two typical online calibration schemes, signal strength difference (SSD) [26] and signal strength ratio (SSR) [19]. SSD and SSR focus on using the pairwise deduction [26] and ratio [19] between AP signals to reduce the effect of device dependency. We also conduct offline RSSI calibration (using linear fitting) [21] to compare with SLAC.

Unless otherwise stated, we use the following parameters as baseline: size of sliding window $M = 7$; number of particles $P = 60$; $\sigma_w = 1$ m for particle weight calculation; η is set to 1.0 in Equation (29); $T = 2$ m in Equation (17). Initially, $[\alpha_{min}, \alpha_{max}, \beta_{min}, \beta_{max}] = [0.1, 1, -0.5, 0]$, $[k_{min}, k_{max}, b_{min}, b_{max}] = [0.1, 6, -10, 0]$. $K = 15$ for FL. For FL, MLL and PFL which may be device and user dependent, we utilize the offline calibration [21, 22] to mitigate heterogeneity effects.

We conduct trials on 5 users with different heights and weights. In experimental trial of airport, we use HTC One X during our site survey and Lenovo A680 as our target devices. In the trial

at the campus atrium, we utilize the HTC One X as survey devices. Then in the target estimation, we use Google Nexus 5 and Lenovo A680.

We evaluate performance of SLAC using following metrics. Let $\mathbf{x}_i$ be target i's true position and $\widehat{\mathbf{x}}_i$ be the estimated location. The mean error (unit:m) of target set $\mathbf{U}$ is given by $\mu_e = \frac{1}{|\mathbf{U}|} \sum_{i=1}^{|\mathbf{U}|} \|\mathbf{x}_i - \widehat{\mathbf{x}}_i\|$. We also evaluate the learning process of SLAC based on dispersiveness (Equation (28)) and the mean localization error.

Illustrative Experimental Results

Figure 8 shows the overall performance of SLAC at baseline parameters in HKIA. Under large signal noise in airport, target RSSI may show similar values with RPs that are distant apart. FL is hence severely influenced by the dispersed nearest neighbors during the fingerprint matching. PFL has not jointly considered the relationship between RSSI and motion information. As the airport contains large indoor open space, particles become too sparse without map constraints, thereof converging slow under large sensor noise. Similarly, MLL

assumes probabilistic independence between different sensor measurements (RF signals and step counter) and also degrades in performance under noisy environment.

Compared with the above state-of-the-art algorithms, SLAC significantly reduces the estimation errors in the indoor large open space. SLAC considers the statistical analysis over wireless RSSI and sensor uncertainty (Equations (2), (6) and (27)). Therefore, SLAC mitigates the influence of uncertainty and thus the localization error decreases. With the joint optimization, SLAC is more robust to signal uncertainty and reduces large localization errors.

Figure 9 shows the weights of RPs in target location estimations. Without joint consideration, the signal noise may lead to a dispersed set of nearest neighbors in signal space. Therefore, the true weight of the physically near RP is diluted and large estimation errors may happen. SLAC, however, jointly considers distance constraints and reduces disperse nearest neighbors, thereof achieving higher localization accuracy.

Figure 10 shows the overtime performance of different algorithms. Under the large signal noise in HKIA, PFL and MLL both degrade in the localization performance. It is because the noisy measurements increase the uncertainty in particle transition and probability distribution, thereof leading to large estimation fluctuation. In contrast, SLAC achieves much smaller localization fluctuation as it considers the correlation among sensors in a joint optimization. It can hence accurately map the target location against the fingerprint map.

Figure 11(a) shows the step counter readings based on repetitive patterns in the accelerometer. Based on the measurement in step counter, SLAC obtains step frequency and walking distance of the user. Figure 11(b) shows the measurement error with respect to the walking distance. T can also be obtained through statistical analysis of above errors (T is set to 2 m in our experiment). Through the calibration in SLAC, we obtain different users' walking parameters and achieve higher accuracy in displacement than uncalibrated step counters.

We also conduct experiment on inexplicit calibration process in SLAC. Figure 12 shows the localization error with respect to time for a target. PFL and MLL do not consider simultaneous localization and calibration. Therefore, if the measured Wi-Fi signals get no pre-calibration, their performance degrades significantly. The localization error of SLAC is high at the first few target samples due to the randomness in RSSI model parameters. Then as the incorrect parameters are filtered, SLAC effectively adapts itself to the device heterogeneity and the error decreases. Therefore, SLAC can learn the heterogeneous model parameters transparently and quickly converge to high localization accuracy.

Figure 13 shows the dispersiveness ξ (Equation (28)) in the learning process under different particle numbers. At the beginning, there are multiple particles at different locations and therefore ξ is large. With particles filtered and RSSI model calibrated, SLAC learns the device parameters and the target estimations converge. Through consistency check, SLAC filters the inconsistent candidates among model parameters and adapts to the device heterogeneity. Clearly, the more
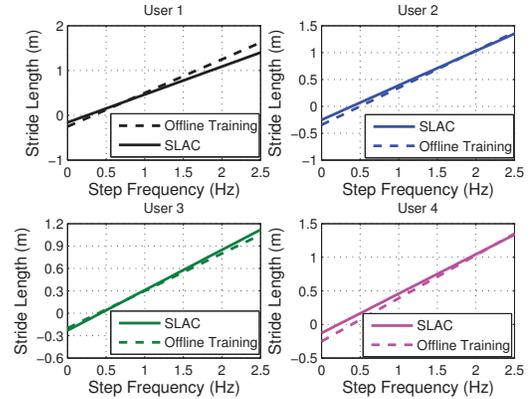
Figure 14. Comparison of step counter calibration performance between SLAC and offline training (airport).

particles, the better learning performance and the slower the convergence as a tradeoff. When ξ is smaller than the defined threshold (as in Equation (29)), fusion is conducted over average parameters (particle number P is set to 1).

Figure 14 shows the step length calibration of SLAC of four different users. We also conduct the offline training using map information to calibrate the step length [18] as comparison. Different from these works using offline training, SLAC learns the parameters using online readings of Wi-Fi and step counter. With simultaneous calibration and localization, SLAC obtains close parameters in step length model with those from offline training. It confirms that SLAC can effectively learn the user parameters through transparent calibration.

Figure 15 shows the localization accuracy between different approaches over device dependency. Both SSD and SSR utilize the online measured RSSI vectors for online calibration. However, under large signal noise, the deduction and ratio between pairwise signals is vulnerable to noise fluctuation. Different from the above approaches, SLAC utilizes the motion information to jointly find the calibration parameters. Therefore, it reduces the influence of noise while achieving higher accuracy and robustness.

Figure 16 illustrates an example of the RSSI calibration. As comparison, offline signal calibration (linear fitting) is also conducted between Lenovo A680 and HTC One X using 60 signal vectors. We can observe that SLAC can achieve close calibration results as the accurate but tedious offline calibration. Therefore, SLAC is capable of online calibration without explicit user participation and tedious offline training.

Figure 17 shows localization error versus number of Wi-Fi temporal targets (i.e., window size M) for SLAC under different particle numbers. As more Wi-Fi samples are jointly considered, the sliding window extends and localization accuracy increases. It is because a larger sliding window reduces uncertainty of overall signal difference with fingerprint map, and the target is more likely to be mapped to an accurate location. The improvement converges after reaching a few temporal targets. Localization accuracy also benefits from more particles due to more accurate parameter estimation.
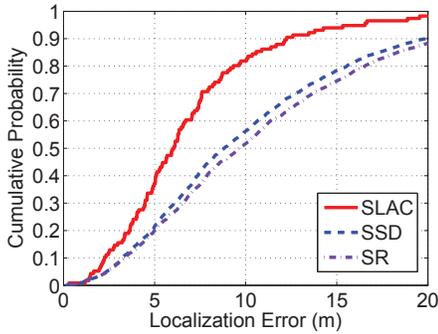
Figure 15. Cumulative errors of algorithms approaching device dependency (airport).
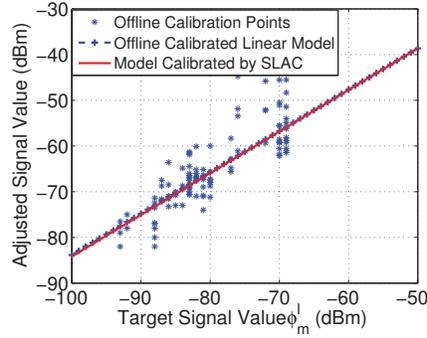
Figure 16. Performance of device calibration using SLAC (airport).
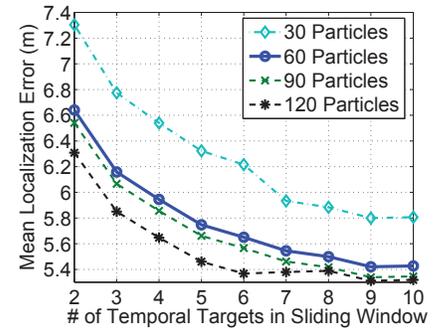
Figure 17. Localization error versus Wi-Fi temporal target number (airport).
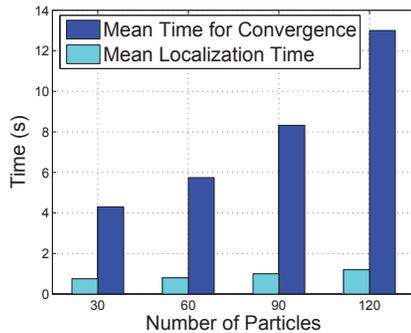
Figure 18. Mean convergence time and mean localization time in SLAC learning (airport).
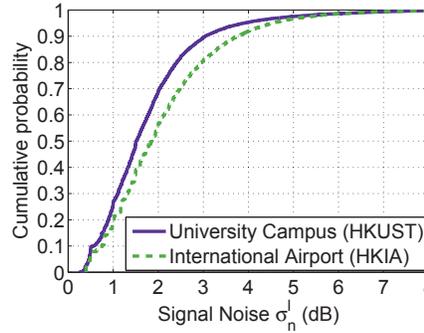
Figure 19. Cumulative probability of the signal noise σ_n^l in the two survey sites.
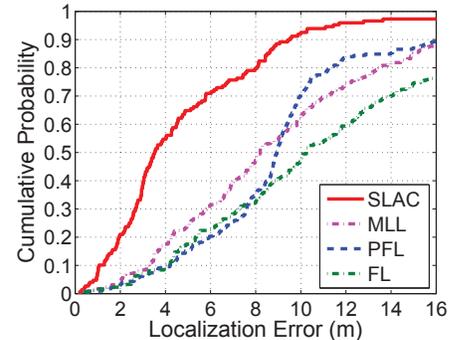
Figure 20. The cumulative probability of localization performance (university atrium).

Figure 18 shows the mean time for convergence in parameter learning (time between system start and final convergence) and localization (time for target position estimation) of SLAC with respect to number of particles. Clearly, as the particle number increases, the longer time SLAC needs for convergence of self-calibration. During the self-calibration, preliminary localization results are simultaneously provided as the user walks. After the convergence, the corresponding profiles can be stored in the database and therefore the self-calibration does not need to be conducted again. To achieve balance between localization accuracy and computational efficiency, we choose $M = 7$ and 60 particles in our experimental settings.

Figure 19 shows the signal noise (σ_n^l in Equation (2)) in the corresponding survey sites. Due to the crowds of people and larger indoor open space, the signals in HKIA show much more fluctuations than in the campus. As shown in Figure 19, the signal noise in the sites can be up to 5 dB in the airport, which may introduce large measurement errors for traditional fingerprint localization. Under such noisy environment, SLAC can still achieve higher accuracy and self-calibration.

We have also conducted the experimental trials in our university atrium at HKUST. Recall that as shown in Figure 4, our atrium has more wall partitions than HKIA. Under wall partition, the fingerprints show more differentiation. In Figure 19, we have also observed smaller signal noise on campus. Thus, we can observe in Figure 20 that SLAC achieves much better performance than in HKIA. Note the marked resemblance between Figure 20 and Figure 8. As the results are qualitatively similar, we do not replicate others for brevity.

CONCLUSION

Step counter has been used to obtain user step frequency and counts, which serves as input to a user-based model to estimate user displacement. The model parameters need to be calibrated for different users due to their different stride length, the so-called user heterogeneity. Given a signal, different devices may report different RSSI readings. These heterogeneous devices hence need to be calibrated to align RSSI measurements. To address user and device heterogeneities when fusing step counter with fingerprints for indoor localization, the traditional approach is to pre-calibrate explicitly the user model and device reading, which is tedious and inconvenient.

We propose SLAC, a novel calibration-free localization framework which simultaneously localizes the target and calibrates the system. SLAC formulates an optimization problem embedded with a specially designed particle filter. The problem jointly considers RSSI calibration and step counter measurement to localize a target with high accuracy. It utilizes the correlation in location estimations, RSSI readings and step information to transparently calibrate devices and user models. We have conducted extensive experimental trials in the Hong Kong International Airport and HKUST atrium. Our results show that SLAC can significantly improve localization accuracy while learning the models for counter and device RSSI.

ACKNOWLEDGMENT

REFERENCES

1. ABI Research 2015. Location Technologies Market Research. (May 2015). `https://www.abiresearch.com/market-research/service/location-technologies/`.

2. M. Sanjeev Arulampalam, Simon Maskell, Neil Gordon, and Tim Clapp. 2002. A tutorial on particle filters for online nonlinear/non-Gaussian Bayesian tracking. *IEEE Trans. Signal Processing* 50, 2 (2002), 174–188.

3. Paramvir Bahl and Venkata N. Padmanabhan. 2000. RADAR: An in-building RF-based user location and tracking system. In *Proc. INFOCOM*, Vol. 2. IEEE, Washington, DC, USA, 775–784.

4. Stephen P Boyd and Lieven Vandenberghe. 2004. *Convex Optimization*. Cambridge University Press, UK.

5. Agata Brajdic and Robert Harle. 2013. Walk detection and step counting on unconstrained smartphones. In *Proc. UbiComp*. ACM, New York, NY, USA, 225–234.

6. Lyu-Han Chen, E.H.-K. Wu, Ming-Hui Jin, and Gen-Huey Chen. 2014. Homogeneous features utilization to address the device heterogeneity problem in fingerprint localization. *IEEE Sensors Journal* 14, 4 (April 2014), 998–1005.

7. Chen Feng, Wain Sy Anthea Au, Shahrokh Valaee, and Zhenhui Tan. 2012. Received-signal-strength-based indoor positioning using compressive sensing. *IEEE Trans. Mobile Computing* 11, 12 (Dec. 2012), 1983–1993.

8. Brian Ferris, Dieter Fox, and Neil D Lawrence. 2007. WiFi-SLAM using Gaussian process latent variable models. In *IJCAI*, Vol. 7. Morgan Kaufmann Publishers Inc., San Francisco, CA, USA, 2480–2485.

9. D. Fox, Jeffrey Hightower, Lin Liao, D. Schulz, and G. Borriello. 2003. Bayesian filtering for location estimation. *IEEE Pervasive Computing* 2, 3 (July 2003), 24–33.

10. Yuan Gao, Qingxuan Yang, Guanfeng Li, Edward Y Chang, Dong Wang, Chengu Wang, Hang Qu, Pei Dong, and Faen Zhang. 2011. XINS: The anatomy of an indoor positioning and navigation architecture. In *Proc. MLBS (UbiComp Workshop)*. ACM, New York, NY, USA, 41–50.

11. Abhishek Goswami, Luis E. Ortiz, and Samir R. Das. 2011. WiGEM: A learning-based approach for indoor localization. In *Proc. CoNext*. ACM, New York, NY, USA, Article 3, 12 pages.

12. Xiaonan Guo, Dian Zhang, Kaishun Wu, and L.M. Ni. 2014. MODLoc: Localizing multiple objects in dynamic indoor environment. *IEEE Trans. Parallel and Distributed Systems* 25, 11 (Nov. 2014), 2969–2980.

13. Dongsoo Han, Sukhoon Jung, Minkyu Lee, and Giwan Yoon. 2014. Building a practical Wi-Fi-based indoor navigation system. *IEEE Pervasive Computing* 13, 2 (2014), 72–79.

14. Robert Harle. 2013. A Survey of Indoor Inertial Positioning Systems for Pedestrians. *IEEE Communications Surveys and Tutorials* 15, 3 (Third 2013), 1281–1293.

15. Suining He and S.-H. Gary Chan. 2014. Sectjunction: Wi-Fi indoor localization based on junction of signal sectors. In *Proc. ICC*. IEEE, Washington, DC, USA, 2605–2610.

16. Suining He and S.-H. Gary Chan. to appear. Wi-Fi fingerprint-based indoor positioning: Recent advances and comparisons. *IEEE Communications Surveys and Tutorials* (to appear).

17. Suining He, S.-H. Gary Chan, Lei Yu, and Ning Liu. 2015. Fusing noisy fingerprints with distance bounds for indoor localization. In *Proc. INFOCOM*. IEEE, Washington, DC, USA, 2506–2514.

18. Sebastian Hilsenbeck, Dmytro Bobkov, Georg Schroth, Robert Huitl, and Eckehard Steinbach. 2014. Graph-based data fusion of pedometer and WiFi measurements for mobile indoor positioning. In *Proc. UbiComp*. ACM, New York, NY, USA, 147–158.

19. Mikkel Baun Kjargaard. 2011. Indoor location fingerprinting with heterogeneous clients. *Pervasive and Mobile Computing* 7, 1 (2011), 31 – 43.

20. Nicholas D. Lane, Emiliano Miluzzo, Hong Lu, Daniel Peebles, Tanzeem Choudhury, and Andrew T. Campbell. 2010. A survey of mobile phone sensing. *IEEE Communications Magazine* 48, 9 (Sept. 2010), 140–150.

21. C. Laoudias, D. Zeinalipour-Yazti, and C.G. Panayiotou. 2013. Crowdsourced indoor localization for diverse devices through radiomap fusion. In *Proc. IPIN*. IEEE, Washington, DC, USA, 1–7.

22. Fan Li, Chunshui Zhao, Guanzhong Ding, Jian Gong, Chenxing Liu, and Feng Zhao. 2012. A reliable and accurate indoor localization method using phone inertial sensors. In *Proc. UbiComp*. ACM, New York, NY, USA, 421–430.

23. Liqun Li, Guobin Shen, Chunshui Zhao, Thomas Moscibroda, Jyh-Han Lin, and Feng Zhao. 2014. Experiencing and handling the diversity in data density and environmental locality in an indoor positioning service. In *Proc. MobiCom*. ACM, New York, NY, USA, 459–470.

24. Hui Liu, Houshang Darabi, Pat Banerjee, and Jing Liu. 2007. Survey of wireless indoor positioning techniques and systems. *IEEE Trans. Systems, Man, and Cybernetics* 37, 6 (2007), 1067–1080.

25. Dimitrios Lymberopoulos, Jie Liu, Xue Yang, Romit Roy Choudhury, Vlado Handziski, and Souvik Sen. 2015. A realistic evaluation and comparison of indoor location technologies: Experiences and lessons learned. In *Proc. IPSN*. ACM, New York, NY, USA, 178–189.

26. A.K.M. Mahtab Hossain, Yunye Jin, Wee-Seng Soh, and Hien Nguyen Van. 2013. SSD: A robust RF location fingerprint addressing mobile devices' heterogeneity. *IEEE Trans. Mobile Computing* 12, 1 (Jan. 2013), 65–77.

27. Youngtae Noh, Hirozumi Yamaguchi, Uichin Lee, Prema Vij, Joshua Joy, and Mario Gerla. 2013. CLIPS: Infrastructure-free collaborative indoor positioning scheme for time-critical team operations. In *Proc. PerCom*, Vol. 18. IEEE, Washington, DC, USA, 172–178.

28. Jun-geun Park, Dorothy Curtis, Seth Teller, and Jonathan Ledlie. 2011. Implications of device diversity for organic localization. In *Proc. INFOCOM*. IEEE, Washington, DC, USA, 3182–3190.

29. Jiuchao Qian, Jiabin Ma, Rendong Ying, and Peilin Liu. 2013. RPNOS: Reliable pedestrian navigation on a smartphone. In *Geo-Informatics in Resource Management and Sustainable Ecosystem*. Springer, 188–199.

30. Anshul Rai, Krishna Kant Chintalapudi, Venkata N. Padmanabhan, and Rijurekha Sen. 2012. Zee: Zero-effort crowdsourcing for indoor localization. In *Proc. MobiCom*. ACM, New York, NY, USA, 293–304.

31. Jochen Seitz, Thorsten Vaupel, Jasper Jahn, Steffen Meyer, Javier Guttiérrez Boronat, and Jörn Thielecke. 2010. A hidden Markov model for urban navigation based on fingerprinting and pedestrian dead reckoning. In *Proc. Fusion*. IEEE, Washington, DC, USA, 1–8.

32. Guobin Shen, Zhuo Chen, Peichao Zhang, Thomas Moscibroda, and Yongguang Zhang. 2013. Walkie-Markie: Indoor pathway mapping made easy. In *Proc. NSDI*. USENIX, Berkeley, CA, USA, 85–98.

33. Wei Sun, Junliang Liu, Chenshu Wu, Zheng Yang, Xinglin Zhang, and Yunhao Liu. 2013. MoLoc: On distinguishing fingerprint twins. In *Proc. ICDCS*. IEEE, Washington, DC, USA, 226–235.

34. Daisuke Taniuchi, Xiaopeng Liu, Daisuke Nakai, and Takuya Maekawa. 2015. Spring model based collaborative indoor position estimation with neighbor mobile devices. *IEEE Journal of Selected Topics in Signal Processing* 9, 2 (March 2015), 268–277.

35. Daisuke Taniuchi and Takuya Maekawa. 2015. Automatic update of indoor location fingerprints with pedestrian dead reckoning. *ACM Trans. Embedded Computing System* 14, 2, Article 27 (Feb. 2015), 23 pages.

36. Yuki Tsuda, Quan Kong, and Takuya Maekawa. 2013. Detecting and correcting WiFi positioning errors. In *Proc. UbiComp*. ACM, New York, NY, USA, 777–786.

37. Mostafa Uddin and Tamer Nadeem. 2014. SpyLoc: A light weight localization system for smartphones. In *Proc. SECON*. IEEE, Washington, DC, USA, 72–80.

38. He Wang, Souvik Sen, Ahmed Elgohary, Moustafa Farid, Moustafa Youssef, and Romit Roy Choudhury. 2012. No need to war-drive: Unsupervised indoor localization. In *Proc. MobiSys*. ACM, New York, NY, USA, 197–210.

39. Hongkai Wen, Zhuoling Xiao, Niki Trigoni, and Phil Blunsom. 2013. On assessing the accuracy of positioning systems in indoor environments. In *Wireless Sensor Networks (Proc. EWSN)*. Lecture Notes in Computer Science, Vol. 7772. Springer Berlin Heidelberg.

40. Oliver Woodman and Robert Harle. 2008. Pedestrian localisation for indoor environments. In *Proc. UbiComp*. ACM, New York, NY, USA, 114–123.

41. Chenshu Wu, Zheng Yang, and Yunhao Liu. 2015. Smartphones based crowdsourcing for indoor localization. *IEEE Trans. Mobile Computing* 14, 2 (2015), 444–457.

42. Kaishun Wu, Jiang Xiao, Youwen Yi, Dihu Chen, Xiaonan Luo, and Lionel M. Ni. 2013. CSI-based indoor localization. *IEEE Trans. Parallel and Distributed Systems* 24, 7 (July 2013), 1300–1309.

43. Zhuoling Xiao, Hongkai Wen, Andrew Markham, and Niki Trigoni. 2014. Lightweight map matching for indoor localisation using conditional random fields. In *Proc. IPSN*. ACM, New York, NY, USA, 131–142.

44. Z. Xiao, H. Wen, A. Markham, and N. Trigoni. 2015. Robust indoor positioning with lifelong learning. *IEEE Journal on Selected Areas in Communications* (2015).

45. Hongwei Xie, Tao Gu, Xianping Tao, Haibo Ye, and Jian Lv. 2014. MaLoc:A practical magnetic fingerprinting approach to indoor localization using smartphones. In *Proc. UbiComp*. ACM, New York, NY, USA, 243–253.

46. Zhice Yang, Zeyu Wang, Jiansong Zhang, Chenyu Huang, and Qian Zhang. 2015a. Wearables can afford: Light-weight indoor positioning with visible light. In *Proc. MobiSys*. ACM, New York, NY, USA, 317–330.

47. Zheng Yang, Chenshu Wu, Zhang Xinglin, Xu Wang, and Yunhao Liu. 2015b. Mobility increases localizability: A survey on wireless indoor localization using inertial sensors. *ACM Comput. Surveys* 47, 3, Article 54 (2015), 34 pages.

48. Zheng Yang, Zimu Zhou, and Yunhao Liu. 2013. From RSSI to CSI: Indoor localization via channel response. *ACM Comput. Surveys* 46, 2, Article 25 (2013), 32 pages.

49. Moustafa Youssef and Ashok Agrawala. 2005. The Horus WLAN location determination system. In *Proc. MobiSys*. ACM, New York, NY, USA, 205–218.

50. Francisco Zampella, Alfonso Bahillo, Javier Prieto, Antonio R. Jimnez, and Fernando Seco. 2013. Pedestrian navigation fusing inertial and RSS/TOF measurements with adaptive movement/measurement models: Experimental evaluation and theoretical limits. *Sensors and Actuators A: Physical* 203, 0 (2013), 249 – 260.

51. Lan Zhang, Kebin Liu, Yonghang Jiang, Xiang-Yang Li, Yunhao Liu, and Panlong Yang. 2014. Montage: Combine frames with movement continuity for realtime multi-user tracking. In *Proc. INFOCOM*. IEEE, Washington, DC, USA, 799–807.

52. Xinglin Zhang, Zheng Yang, Longfei Shangguan, Yunhao Liu, and Lei Chen. 2015. Boosting mobile Apps under imbalanced sensing data. *IEEE Trans. Mobile Computing* 14, 6 (June 2015), 1151–1161.

53. Wiebren Zijlstra. 2004. Assessment of spatio-temporal parameters during unconstrained walking. *European Journal of Applied Physiology* 92, 1-2 (2004), 39–44.